Speckle Reduction Performance Estimation

Fergal Shevlin

DYOPTYKA, Dublin, Ireland.

ABSTRACT

This study introduces an approach for estimating the speckle reduction performance of our technology at high frequencies, using measurements of speckle contrast made at lower frequencies. Results demonstrate the scaling of speckle contrast with cumulative exposure period. We propose a fitting model for initial speckle contrast and approximate contrasts for extended exposure periods based on the model.

Keywords: Speckle reduction, deformable mirror, high frequency.

1. INTRODUCTION

Our company's phase-randomizing deformable mirror (DM) technology[1] achieves speckle reduction with excellent optical efficiency and at temporal frequencies orders of magnitude higher than alternative techniques such as moving diffusers and shaking fibers, see figure 1. However its speckle reduction performance at such high frequencies is difficult to predict because speckle reduction is not solely a function of frequency; characteristics of the coherent source, the illumination optical system, and the imaging optical system all influence the generation of uncorrelated speckle patterns. Herein we describe an approach to high frequency performance estimation that requires only careful measurement of speckle contrast arising from any spatio-temporal averaging technique at lower temporal frequencies.

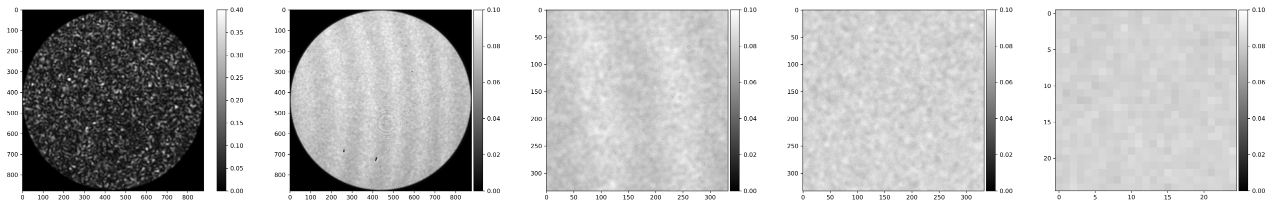

Figure 1. [Left pair] Exit face of ⌀200 µm 0.22 N.A. multimode fiber acquired with 20 µs sensor exposure period; with DM inactive and active at approx. 1.5 MHz, speckle contrast ratio $C_S \approx 59.2\%$ and $C_S \approx 5.6\%$ respectively. [Center] Region of image with DM active, showing interference fringes from protective window of sensor. [Right pair] The same region with fringes subtracted in the process described in Section 2, $C_S \approx 4.1\%$; and with fringes subtracted and downsampled by 13× to simulate a sensor resolution equal to the optical resolution of the apparatus, $C_S \approx 2.1\%$.

2. APPARATUS

The fiber-coupled apparatus used for experimentation is described in figure 2. Investigation of the interference fringes visible in figure 1 found them to be relatively stable over multiple image exposures once the camera was clamped tightly to minimize vibration. Since they prevented accurate measurement of low values of speckle contrast we determined to remove them through image processing. For each exposure period of interest, we averaged a set of 25 images acquired with DM active, subtracted the mean image from each, and added the mean intensity. We used the processed image set for the experimentation described in section 3.

The investigation also revealed a variety of relatively stable Airy disc-like objects of size similar to the expected diffraction-limited spot size of the multimode fiber collimator. We considered downsampling the imagery to compensate for sensor resolution being approx. 13× higher than optical resolution. We concluded that it was not necessary to do so because the objects were also removed through the aforementioned image processing.

E-mail address: fshevlin@dyoptyka.com. Postal address: 7 Westland Court, South Cumberland St., Dublin 2, Ireland.

PREPRINT for Laser Display and Lighting Conference, Yokohama, April 22-26, 2024.

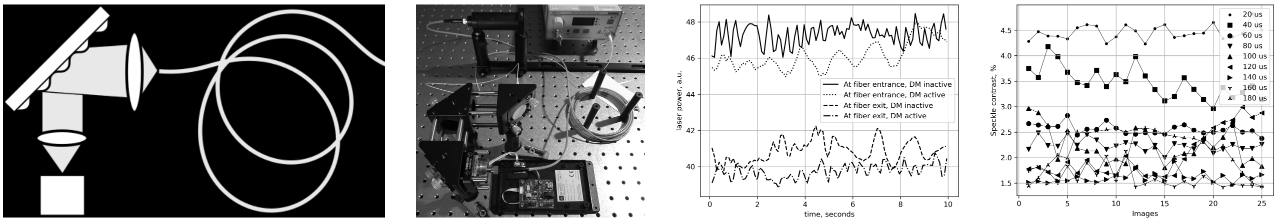

Figure 2. [First] Light from the laser source is directed onto the DM from where it is reflected with randomized divergence and focused into the entrance face of multimode optical fiber. [Second] Thorlabs S4FC520 Fabry-Perot 520 nm CW laser source with narrow linewidth coupled into single mode optical fiber terminated with a collimator to form an approx. ⌀1 mm beam directed onto a Dyoptyka DM from where a Thorlabs PAF2S-7A couples into a 2 m length of ⌀200 µm, 0.22 N.A. multimode fiber terminated with a Thorlabs F220SMA-A collimator to project an image of the fiber exit face directly onto the 1920×1200 pixel sensor of a Basler acA1920 monochrome camera (not shown.) [Third] Power meter measurements showing approx. 85% efficiency of coupling and transmission through the multimode fiber. Higher efficiency is possible with optimized coupling. [Fourth] Speckle contrast ratios calculated from images acquired with different exposure periods. Variations likely due to not all sequences of random deformations on the DM resulting in uncorrelated speckle patterns.

3. EXPERIMENTATION

Figure 3 [Left] shows how the speckle contrast of the averages of up to 25 images scales in accordance with theory. Figure 3 [Center] shows the fit to cumulative exposure periods rather than to image count. To improve the quality of the fit we diversified the observations and increased their number to 68 by acquiring multiple images over a range of different exposure periods. Figure 3 [Right] Shows in more detail the extrapolated values of speckle contrast the shortest observed exposure period of 20 µs and that fitted for 1 µs.

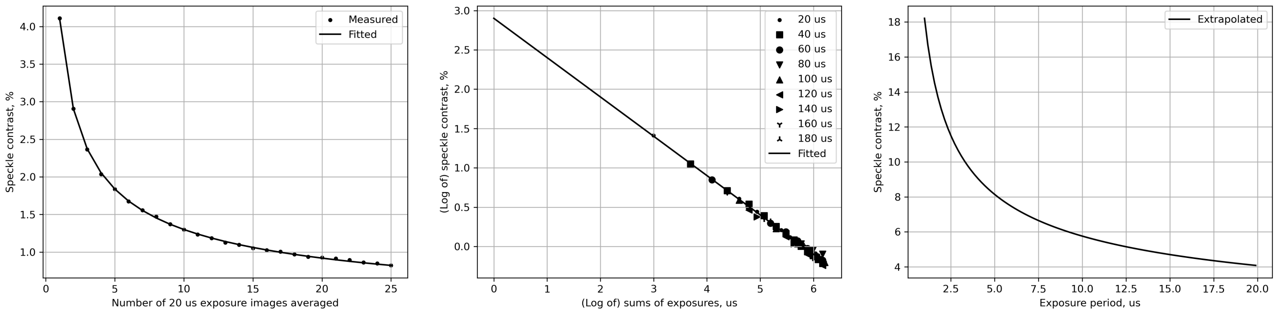

Figure 3. [Left] Speckle contrast ratios calculated from the averages of an increasing number of 20 µs exposure images show a good fit to the theoretical $a/\sqrt{n}$ for an initial contrast a and n uncorrelated speckle patterns.[2] [Center] Contrasts calculated from increasing numbers of images until their sums of exposures reach 500 µs, with $b/\sqrt{m}$ fit, for initial contrast b and cumulative exposure period m. [Right] Extrapolated range between 20 µs and 1 µs in more detail.

4. CONCLUSIONS

We propose that the initial speckle contrast achievable with our technology be approximated by coefficient b of the least squared error fit of $b/\sqrt{m}$ to measured speckle contrast ratios with cumulative exposure period m, and that contrasts for longer exposure periods (or pulse lengths) can approximated in accordance with the fit.

REFERENCES

[1] Shevlin, F., "Phase randomization for spatio-temporal averaging of unwanted interference effects arising from coherence," *Applied Optics* **57**(22), E6–E10 (2018).

[2] Goodman, J., [*Speckle phenomena in optics*], Roberts and Company, Colorado, USA (2007).